analytical chemistry

Article

pubs.acs.org/ac

Toward Full Spectrum Speciation of Silver Nanoparticles and Ionic Silver by On-Line Coupling of Hollow Fiber Flow Field-Flow Fractionation and Minicolumn Concentration with Multiple Detectors

Zhi-Qiang Tan,[†] Jing-Fu Liu,[*,†,‡] Xiao-Ru Guo,[†] Yong-Guang Yin,[†] Seul Kee Byeon,[§] Myeong Hee Moon,[§] and Gui-Bin Jiang[†,‡]

[†]State Key Laboratory of Environmental Chemistry and Ecotoxicology, Research Center for Eco-Environmental Sciences, Chinese Academy of Sciences, Beijing 100085, China

[‡]Institute of Environment and Health, Jianghan University, Wuhan 430056, China

[§]Department of Chemistry, Yonsei University, Seoul 120-749, Korea

Supporting Information

ABSTRACT: The intertransformation of silver nanoparticles (AgNPs) and ionic silver (Ag(I)) in the environment determines their transport, uptake, and toxicity, demanding methods to simultaneously separate and quantify AgNPs and Ag(I). For the first time, hollow fiber flow field-flow fractionation (HF5) and minicolumn concentration were on-line coupled together with multiple detectors (including UV–vis spectrometry, dynamic light scattering, and inductively coupled plasma mass spectrometry) for full spectrum separation, characterization, and quantification of various Ag(I) species (*i.e.*, free Ag(I), weak and strong Ag(I) complexes) and differently sized AgNPs. While HF5 was employed for filtration and fractionation of AgNPs (>2 nm), the minicolumn packed with Amberlite IR120 resin functioned to trap free Ag(I) or weak Ag(I) complexes coming from the radial flow of HF5 together with the strong Ag(I) complexes and tiny AgNPs (<2 nm), which were further discriminated in a second run of focusing by oxidizing >90% of tiny AgNPs to free Ag(I) and trapped in the minicolumn. The excellent performance was verified by the good agreement of the characterization results of AgNPs determined by this method with that by transmission electron microscopy, and the satisfactory recoveries (70.7–108%) for seven Ag species, including Ag(I), the adduct of Ag(I) and cysteine, and five AgNPs with nominal diameters of 1.4 nm, 10 nm, 20 nm, 40 nm, and 60 nm in surface water samples.

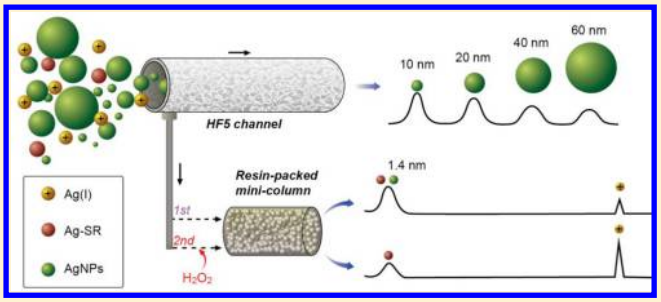

With the development of nanoscience and nanotechnology, the environmental effects and biological safety of nanomaterials, especially engineered nanomaterials, have drawn great interest.[1−4] Silver nanoparticles (AgNPs), as one of the most widely used nanomaterials, play an important role in a variety of fields, including personal care products, clothes, paints, foods, and pharmaceuticals.[5] The widespread use of AgNPs leads to their inevitable discharge into domestic wastewater and their entrance into wastewater treatment plants (WWTP), which could threaten natural bacterial communities.[6,7]

Given the highly dynamic properties of AgNPs, it is believed that AgNPs and ionic silver (Ag(I)) are coexisting and undergo intertransformation in the environment. Their chemical and morphological transformations would influence their fates and behaviors in the natural environments. It was evidenced that AgNPs were prone to transforming into other silver species, such as Ag(I).[8−10] The cooperative oxidation process in the presence of dissolved oxygen and protons could lead to release of Ag(I); thus, AgNPs and Ag(I), including free Ag(I) and its complexes, commonly coexisted in even simple AgNPs colloids.[11] On the contrary, Ag(I) in natural water could be reduced to AgNPs by the superoxide from phenol groups in natural organic matter (NOM) under sunlight,[12] and both AgNPs and Ag(I) were not thermodynamically stable, resulting in the simultaneous occurrence of reduction of Ag(I) into AgNPs and oxidative dissolution of AgNPs in sunlit NOM-rich water.[13] In the WWTP system, the majority of Ag(I) would transform into the thiol-containing strong Ag(I) complexes (Ag-SR) or Ag_2S nanoparticles (Ag_2S NPs)[14] and, therefore, reduced their toxicity as Ag-SR and Ag_2S NPs, which were considered to be much less toxic than Ag(I).[15] In addition, the environmental fate and toxicity of AgNPs were closely related to the size, as smaller AgNPs had a faster release rate of Ag(I)

Received: May 15, 2015
Accepted: July 29, 2015
Published: July 29, 2015

DOI: 10.1021/acs.analchem.5b01827
Anal. Chem. 2015, 87, 8441−8447

due to their high surface area.[10,16] In evaluating the cytotoxicity of AgNPs in human cells, the half effective concentration was found to be dependent on the size of AgNPs, and the smaller AgNPs showed higher toxicity, since they could enter cells more easily than the larger ones.[17] Very recently, we showed that free Ag(I) was the intrinsic and ultimate factor that governed the acute toxicity of AgNPs to *D. magna*, while size and surface coating were apparent factors that influenced the toxicity through affecting the free Ag(I) concentration.[18] Therefore, to assess the AgNPs-related risks, the foremost step is to develop effective and reliable methods to characterize and quantify different Ag species, including different sized AgNPs and Ag(I) in the environment.

A series of methods have been developed for separation and size characterization of nanomaterials,[19] including centrifugation[20] and extraction[21,22] followed by microscopy-based techniques, size exclusion chromatography,[23,24] capillary electrophoresis,[25] and flow field-flow fractionation (flow FFF).[26] Among these methods, centrifugation and extraction are the simplest methods for separating nanoparticles and small molecules or ions, but they are seldom used to separate nanomaterials with a wide size distribution.[27] Size exclusion chromatography was successfully used to characterize nanomaterials with a wide size distribution, but the irreversible adsorption of nanoparticles (NPs) onto the column should be prevented by using a suitable mobile phase.[28] Capillary electrophoresis shows the capability to separate charged NPs, but the separation mechanism is based upon the electrophoretic mobility, which is dominated by the surface charge density and radius of the particle, as well as the thickness of the electric double layer,[28,29] making the characterization of particle size very complicated.

Without a stationary phase in the channel, flow FFF is nearly interaction free and capable of size-sorting AgNPs in the sub-10 nm regime.[26] As an alternative, hollow fiber flow FFF (HF5), known as the third type of flow FFF, has been developed as a well-established technology to separate colloidal particles and macromolecules.[30,31] Since the spearheaded investigations by Lee et al.[32] and further improvement by Jönsson's group,[33] HF5 has been extensively applied in the analysis of synthetic polymers, cells, bacterial, and biological macromolecules.[34−37] In fractionation, the target is first driven toward the HF wall under the radial flow and located at the equilibrating position, and then it moves along the HF channel under the axis flow to the detector at different speeds according to the difference in size. In addition to comparable separation ability with conventional flow FFF, HF5 employing inexpensive and disposable HF as a focusing/relaxation channel is featured with low cost, miniaturization, in-line cleanup of sample, and simple installation and operation. Considering the similar operating flow rate of flow FFF and the inductively coupled plasma mass spectrometer (ICPMS) sample introduction, ICPMS as a sensitive element detector has a great potential to be coupled with flow FFF for measurement of the size-resolved elemental composition of AgNPs.[38−40] However, to the best of our knowledge, as Ag(I) and tiny AgNPs (e.g., <2 nm) are inevitably filtered through the membrane pores in fractionation, it remains a great challenge to simultaneously analyze AgNPs over a wide range of sizes and Ag(I) by HF5.

In this study, a novel method based on on-line coupled HF5 and minicolumn concentration (MCC) with UV−vis spectrometry (UV)/dynamic light scattering (DLS)/ICPMS was developed for the first time for separation, characterization, and quantification of both AgNPs and Ag(I) in aqueous matrices. The HF5, the key part of the system, was developed to fractionate AgNPs with sizes >2 nm. The Ag(I) from the radial outlet of the HF5 part was separated into two fractions; namely, the free Ag(I) or weak Ag(I) complexes were concentrated by adsorption onto the minicolumn packed with Amberlite IR120 resin, and the strong complexed Ag(I) such as Ag-SR that cannot be adsorbed onto the Amberlite IR120 resin was delivered directly into the detector. The tiny AgNPs (<2 nm) with size less than the HF pore diameter (∼2 nm) would be filtered together with Ag-SR. Discriminating strong Ag(I) complexes and tiny AgNPs was conducted in a second run of focusing by oxidizing >90% of tiny AgNPs to free Ag(I) and trapping them in the minicolumn. The UV−vis spectrometer was used to record AgNPs and size standard polystyrene nanoparticles (PS NPs) for size characterization, DLS was applied to measure the hydrodynamic diameter of the AgNPs, and ICPMS was employed to provide mass concentration information.

EXPERIMENTAL SECTION

Chemical and Materials. Standard stock solutions of Ag(I) (GSB04−1712−2004) were obtained from the National Institute of Metrology (Beijing, China). Four commercial stock colloids of citrate-coated AgNPs with nominal diameters of 10, 20, 40, and 60 nm at concentration of 0.02 mg/mL and L-cysteine (Cys, ≥ 98.5%) were purchased from Sigma-Aldrich (St. Louis, MO). Working solutions of Ag(I) and AgNPs were prepared by sequential diluting stock standard solution with the mobile phase solution. PS NPs with certified diameters of 22 ± 2 nm, 46 ± 2 nm, and 100 ± 3 nm, respectively, were purchased from the National Institute of Standards and Technology (NIST, Gaithersburg, MD). Surfactant FL-70 was purchased from Thermo (Fair Lawn, NJ). Sodium thiosulfate ($Na_2S_2O_3$), ammonium pyrrolidinedithiocarbamate (APDC), and glutathione (GSH) were from Sigma-Aldrich (St. Louis, MO), and sodium azide (NaN_3) as the bactericide was from Ameresco (Framingham, MA). Sodium tetraborate ($NaBH_4$) was bought from Tianjin Jinke Fine Chemical Institute (Tianjin, China). Other chemicals such as $NaClO_4$, $AgNO_3$, ammonium hydroxide (NH_4OH), disodium ethylenediaminetetraacetic acid (EDTA), sodium citrate, and sodium diethyldithiocarbamatre (DDTC) bought from Sinopharm Chemical Reagent Co. (Shanghai, China) were with purity of at least of analytical grade. High purity water (18.3 MΩ) produced with a Milli-Q Gradient system (Millipore, Bedford) was used throughout the whole study.

Amberlite IR120 resin in sodium form, composed of styrene divinylbenzene copolymer matrix and with particle size of 0.3−1.2 mm (≥95%), exchange capacity of 4.2 mmol/g and wet water content of 40−50%, was bought from Sinopharm Chemical Reagent Co. (Shanghai, China). The poly(ether sulfone) (PES) HF with dimensions of 0.80 mm × 1.40 mm × 24 cm (I.D. × O.D. × length) and a nominal molecular mass cutoff of 10 kDa were obtained from Kaihong Membrane Technology Co., Inc. (Hangzhou, China) and used for constructing the HF5 channel module. Lake water and river water samples were collected from Gaobeidian lake (Beijing, China) and Chaobai river (Beijing, China), respectively.

System Setup. Figure 1 illustrates the scheme of the developed HF5/MCC-UV/DLS/ICPMS system. A model 1200 high performance liquid chromatography (HPLC) pump (Agilent Technologies, Palo Alto, CA) (Pump 1) was

DOI: 10.1021/acs.analchem.5b01827
Anal. Chem. 2015, 87, 8441−8447

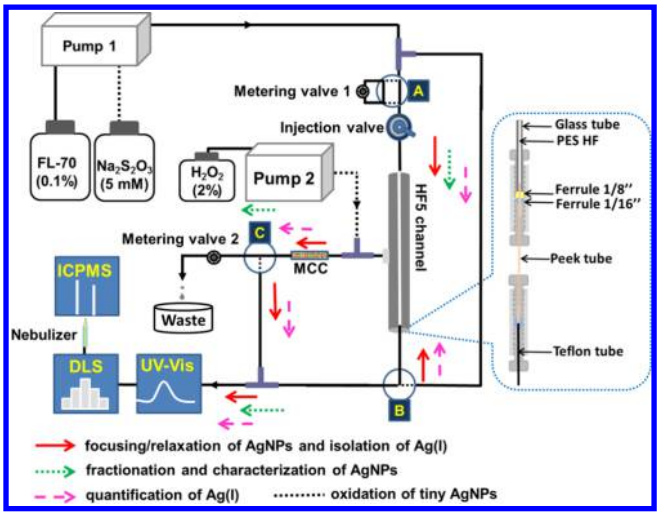

Figure 1. Schematic representation of the on-line coupled HF5/MCC-UV/DLS/ICPMS system. A, four-way valve; B and C, three-way valve. The whole process consisted of three programmable steps, including focusing/relaxation of AgNPs and isolation of Ag(I) (red arrow), fractionation, characterization, and quantification of AgNPs (green arrow), and quantitation of Ag(I) (rose red arrow), which were triggered in sequence.

employed to deliver the mobile phase in the axial direction, and a peristaltic pump (Lange constant flow pump Co., Baoding, China) defined as Pump 2 was used to deliver the diluted H_2O_2 to oxidize the tiny AgNPs (<2 nm) filtered through the HF membrane pores. The HF5 fractionation system, constructed as described in early reports,[34,41] facilitates the separation of Ag(I) and AgNPs and further fractionation of AgNPs according to the size. In brief, an HF was encapsulated in an empty glass column (2.0 mm × 2.3 mm × 20 cm, I.D. × O.D. × length). Into both ends of the fiber was inserted a Teflon tubing, which connected with the polyetheretherketone (PEEK) tubing outside using a union at the one end and a tee at the other. The tee piece was used to provide an outlet for the radial flow. One four-way valve and two three-way valves electronically controlled valves (all from EH4C3WE, VICI, Valco Co., Houston, TX) were used for switching among the focusing/relaxation, fractionation and desorption modes. Two metering valves (SS-31RS4, Nupro, Willoughby, OH) were employed to control the inlet and radial flow rates, respectively. All the units in the hyphenation system were connected through the PEEK tubing (0.50 mm × 1.58 mm, I.D. × O.D.), except that the connection between HF5 system and ICPMS (7700, Agilent Technologies, Palo Alto, CA) was achieved by a commercial concentric nebulizer (MicroMist, Glass Expansion Pty. Ltd., Victoria, Australia). The instrumental parameters of DLS (ZEN3600, Malvern, UK) were referred to the default value. Main parameters for UV−vis spectrometer (1200 series, Agilent Technologies, Palo Alto, CA) and ICPMS were listed in Table 1.

The MCC part made of a glass minicolumn (2.0 mm × 2.3 mm × 10 cm, I.D. × O.D. × length) was packed with 100 mg Amberlite IR120 resin as sorbent for Ag(I) flowing from the radial outlet of the HF5 part. The resin was cleaned using 5% NaCl (w/v), 1 M NaOH, 0.1 M $Na_2S_2O_3$, and ultrapure water in sequence, and activated in 0.01 M NaOH aqueous medium for 24 h.

Operation Procedures. The whole operation procedure consisted of three-step run cycles, including focusing/relaxation of AgNPs and isolation of Ag(I) (red arrow), fractionation, characterization and quantification of AgNPs (green arrow), and quantitation of Ag(I) (rose red arrow), which were triggered in sequence.

Table 1. UV-Vis Spectrometer and ICPMS Operating Parameters for Ag Detection

UV−vis spectrometer	Agilent 1200 VWD
Wavelength	410 nm for AgNPs, 254 nm for PS NPs
ICPMS	Agilent 7700
RF Power	1500 W
Nebulizer flow rate	0.40 mL/min
Plasma gas flow rate	15 L/min
Dwell time	500 ms
Isotopes monitored	^{107}Ag

Focusing/Relaxation of AgNPs and Isolation of Ag(I). Focusing/relaxation of AgNPs and isolation of Ag(I) was fulfilled in the injection/focusing step of the HF5 system modified from Moon group reports.[30,34] Briefly, the HPLC pump was used to provide the required channel flow rates of mobile phase (aqueous solution of 0.1% (v/v) FL-70 and 0.02% (w/v) NaN_3). Valve A was switched to metering valve 1 direction (dotted line in Figure 1), valve B was switched to the HF direction, and valve C was changed to the detector direction. The mobile phase was divided into two parts by a tee connector located before valve A, and metering valve 1 was used to adjust the ratio of V_{in} and V_{out} to be 1:9, where V_{in} and V_{out} represent flow rates of entering the inlet and the outlet of the HF, respectively. Samples were introduced into the system through the inlet of HF by an injection valve (model 7725i, Rheodyne, Rohnert Park, CA) equipped with a 100-μL loop. During focusing, AgNPs of >2 nm was axially compressed and remained in the HF, while the Ag(I) and tiny AgNPs (<2 nm) were dialyzed through the pores of HF membrane and directed to the minicolumn, in which free Ag(I) or weak Ag(I) complexes would be adsorbed onto the Amberlite IR120 resin through ion-exchange with Na(I); and strong complexed Ag(I) (e.g., Ag-SR) together with tiny AgNPs, which were unfavorable for the adsorption by the resin, were transferred directly to the detectors, and total amount of the two species could be quantified. In a second run, introduction of H_2O_2 between the radial outlet of the HF channel and the inlet of the MCC part could achieve oxidation of tiny AgNPs to Ag(I), which could be adsorbed by the resin. Therefore, only the strong complexed Ag(I) was transferred to the detector in the focusing step and quantified. Thus, respective quantification of the tiny AgNPs and the strong complexed Ag(I) was fulfilled based on the difference of the detected Ag amount in the focusing step of the two runs. After focusing for 3−5 min, unfiltered AgNPs was concentrated at the predicted position 1/10 length of the HF (away from the inlet), and nearly all the Ag(I) and tiny AgNPs were filtered out.

Fractionation, Characterization, and Quantification of AgNPs. The fractionation step was triggered by changing configurations of valve A to the HF direction directly (solid line in Figure 1), valve B to the detector direction and valve C to the waste direction. The radial flow rate was set at desired value using metering valve 2. In this step, the fractionated AgNPs species were carried by the axial flow to the multiple detectors (UV/DLS/ICPMS) for identification of particle species, size characterization and quantification.

Quantification of the Free Ag(I). After fractionation, valve A and B were switched back to the original state, and valve C to

DOI: 10.1021/acs.analchem.5b01827
Anal. Chem. 2015, 87, 8441−8447

the detector direction again. Aqueous solution of 5 mM $Na_2S_2O_3$ delivered by the HPLC pump was used as the eluent to desorb and transport the concentrated Ag(I) in the minicolumn to the ICPMS for quantification. After that, the HF channel was flushed with mobile phase at 1.0 mL/min for another 5 min to prevent carryover contamination from the former run. All experiments have been conducted at least in triplicate, and final values were obtained through trial-and-error determination.

Identification of Ag(I) and AgNPs. Ag(I) can be easily identified by the retention time (t_R). AgNPs was comprehensively identified by t_R in fractograms based on UV−vis spectra and ICPMS spectra. Unlike AgNPs with characteristic absorbance peak at around 410 nm in UV−vis spectra, Ag(I) only possess Ag response in ICPMS spectra.

On-Line Characterization of Particle Size. For AgNPs with high concentration, the hydrodynamic particle size was measured directly from the DLS recording. Furthermore, the diameter of AgNPs could also be calibrated based on the t_R in fractograms. For AgNPs with significant signal absorbance peak at around 410 nm in UV−vis spectra, the diameter was precisely measured with a calibration curve prepared by plotting the t_R measured under the same fractionation conditions against the known diameters of standard PS NPs.

Quantification of Ag(I) and AgNPs. Ag(I) was quantified using an external calibration curve prepared by conducting the same operation procedures of samples with Ag(I) standard solutions (5−5000 μg/L) and plotting the ICPMS response against Ag(I) concentration. Given the size-dependent ICPMS response of AgNPs,[42] the concentration of a specific particle size can be quantified with AgNPs of the same species and size, whereas AgNPs with no corresponding standards cannot be directly quantified in this study. The total content of AgNPs in sample can be calculated by the difference of total Ag and Ag(I).

Off-line Characterization of AgNPs. The particle diameter of GSH-protected Ag nanoclusters prepared (details in Supporting Information) and four commercial AgNPs with nominate diameters of 10, 20, 40, and 60 nm and were preliminarily off-line characterized by transmission electron microscope (TEM, 2100F, JEOL, Japan). TEM samples were prepared by dropping 5 μL aliquots of the AgNPs solution onto a carbon coated copper grid and drying in a vacuum desiccator (DZF 6090, Yiheng Technology Co., Ltd., Shanghai, China) overnight at room temperature. TEM results illustrated that the mean diameter of four commercial AgNPs were slightly smaller than those provided by the producer (Figure S1B−E).

RESULTS AND DISCUSSION

Optimization of the HF5 System. An on-line coupled HF5/MCC-UV/DLS/ICPMS system was developed in this study, and the optimization of the HF5 parameters was conducted with two working solutions of 10 and 20 nm AgNPs. Separation resolution and peak area were used to evaluate the fractionation capability of the proposed HF5/MCC-UV/DLS/ICPMS system. The resolution of separation, R_s, was calculated according to eq 1[43]

$$R_s = 2(t_{R2} - t_{R1})/(W_1 + W_2) \quad (1)$$

where t_{R1} and t_{R2} are the retention times of the two near peaks, and W_1 and W_2 are the peak widths at the baseline.

In this study, the aqueous solution of FL-70 was utilized as the mobile phase to stabilize AgNPs in the flow FFF channel. It was found that the separation resolution of the two AgNPs (10 and 20 nm) increased slowly with the increment of FL-70 concentration in the range of 0.01−0.5% (v/v) (Supporting Information, Figure S2). As FL-70 is a mixture of salt (e.g., sodium carbonate) and surfactant (*e.g.*, oleic acid, polyoxyethylene alcohols and poly(ethylene glycol) (Technical Note, Chemistry Division, Fisher Scientific Co.), the change in separation resolution might be attributed to the variation of ionic strength and surfactant. To some extent, the ionic strength in the media dominates the electrical double layer of both nanoparticles and channel wall, which controls the particle−particle and particle−wall interactions.[44] To verify the effect of ionic strength, $NaClO_4$ solutions with various concentrations (0−1%, w/v) were introduced into the system. Results showed that addition of $NaClO_4$ had little impact on both separation resolution and peak widths, except for the slight decrease in t_R. Therefore, surfactants in FL-70 might comprehensively function to disperse AgNPs,[30] which was in favor of improving separation resolution.

Other main variables (i.e., radial flow rate, focusing time, axial flow rate, and sample volume) affecting the separation resolution and ICPMS response were further systematically studied. The optimized conditions were as follows: followed by injection of 100 μL of sample, the focusing step was carried out with a single pump by delivering the mobile phase at the flow rate of 0.70 mL/min into both the inlet and outlet of HF. After 4 min, the fractionation step was performed with the radial flow rate and axial flow rate at 0.70 and 0.80 mL/min, respectively (for details see Figures S3−6 in the Supporting Information).

Optimization of the MCC System. The function of the MCC part was to trap free Ag(I) and weak Ag(I) complex. Thus, this part was optimized by evaluating the recovery of Ag(I) that was calculated by the ratio of the signals (peak area) obtained by the HF5/MCC-UV/DLS/ICPMS system and direct injection into ICPMS (Agilent 7700) without HF5/MCC. To efficiently concentrate the free Ag(I) (100 μL, 2000 μg/L) onto the minicolumn, the amount of Amberlite IR120 resin packed in the column was optimized in the range of 50−200 mg, and it was found that 100 mg of resin was enough to trap >95% of the injected free Ag(I). Considering that a larger amount of resin might prolong the eluting time, 100 mg of resin was chosen to adsorb Ag(I) onto the minicolumn.

Seven conventional Ag(I) complexing agents, including NH_4OH, $Na_2S_2O_3$, Cys, sodium citrate, EDTA, APDC, and DDTC, were tested as the eluent for desorbing Ag(I) from the resin, respectively. The results showed that $Na_2S_2O_3$ provided the highest recovery of Ag(I). We further evaluated the effects of the concentration and flow rate of $Na_2S_2O_3$ on the desorption of Ag(I) (Figure 2). The recovery of Ag(I) increased with $Na_2S_2O_3$ concentration from 0.5 to 5 mM but decreased at over 10 mM. The reduced apparent recovery of Ag(I) might be because a high concentration $Na_2S_2O_3$ could interfere with the subsequent ICPMS detection of Ag. For 5 mM $Na_2S_2O_3$, the recovery of Ag(I) increased with the eluting flow rate up to 1.0 mL/min and then slowly decreased with a further increase of flow rate. Consequently, 5 mM $Na_2S_2O_3$ at a flow rate of 1.0 mL/min was adopted as the optimum in the desorption step.

In view of the employed HF having a nominal molecular mass cutoff of 10 kDa, it was inevitable that tiny AgNPs with diameter <2 nm could be filtered out of the HF5 channel together with Ag(I) in the focusing step.[45] Therefore, it is very important to distinguish tiny AgNPs from Ag(I). Experiments

DOI: 10.1021/acs.analchem.5b01827
Anal. Chem. 2015, 87, 8441−8447

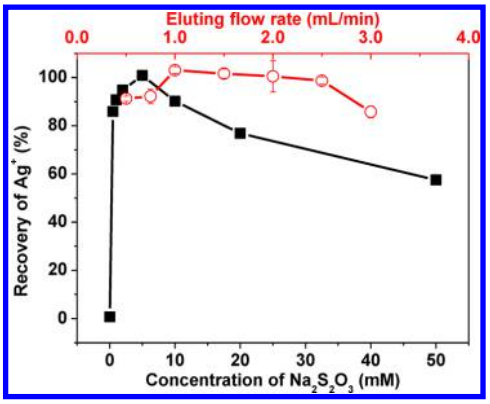

Figure 2. Effects of $Na_2S_2O_3$ concentration and elution flow rate on the recovery of Ag(I). Experimental conditions: sample, 100 μL of 200 μg/L Ag(I); mobile phase, 0.1% (v/v) FL-70 with 0.02% (w/v) NaN_3; inlet flow rate, 1.50 mL/min; radial flow rate, 0.70 mL/min; axial flow, 0.80 mL/min; focusing time, 4 min; resin mass, 100 mg.

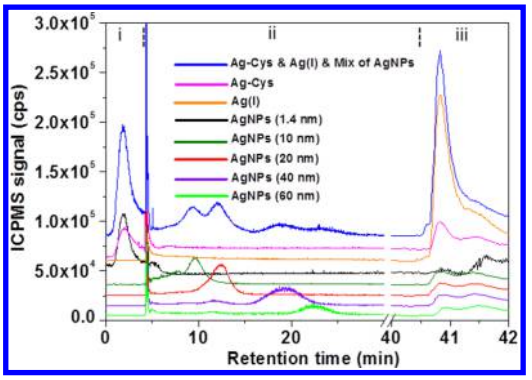

Figure 3. Overlaid elution profiles of individual and mixed samples of Ag(I) and AgNPs by HF5 with ICPMS detection. Experimental conditions: sample, 100 μg/L of each of the Ag species; sample volume, 100 μL; mobile phase, 0.1% (v/v) FL-70 with 0.02% (w/v) NaN_3; inlet flow rate, 1.50 mL/min; radial flow rate, 0.70 mL/min; axial flow, 0.80 mL/min; focusing time, 4 min. Operation procedures: focusing/relaxation of AgNPs and isolation of Ag(I) (i), fractionation, characterization and quantification of AgNPs (ii), and quantitation of Ag(I) (iii).

showed that tiny AgNPs (1.4 nm) were not trapped in the minicolumn (data not shown), possibly due to the fact that the AgNPs studied were negatively charged and decline to be adsorbed onto the Amberlite IR120 resin in the minicolumn. Thus, tiny AgNPs were directly delivered to the detector and quantified together with strong Ag(I) complexes (e.g., Ag-SR) that could not be trapped by the Amberlite IR120 resin either. To quantify the tiny AgNPs and strong Ag(I) complexes, respectively, we conducted a second run in which H_2O_2 (2%, v/v) was introduced into the flow through a tee joint between the radial outlet of the HF and the inlet of the MCC part at the same flow rate with the radial flow, to selectively oxidize the tiny AgNPs into free Ag(I) that was trapped by the Amberlite IR120 resin in the minicolumn, while the Ag-SR was delivered to the ICPMS and quantified. Experiments showed that introduction of 2% H_2O_2 is able to effectively oxidize over 90% of the tiny AgNPs into Ag(I), while the Ag-SR remained unchanged. Therefore, the concentration of tiny AgNPs, if any, could be calculated from the decrement of the detected Ag amount in the focusing step of the two runs.

Performance of the Developed System. *Separation of Ag(I) and AgNPs.* Figure 3 shows the HF5 elution profiles of the mixture and individual working solution of seven Ag species (i.e., Ag(I), the adduct of Ag(I) and Cys (Ag-Cys), and five AgNPs with nominal diameters of 1.4, 10, 20, 40, and 60 nm; each at 100 μg/L) recorded by ICPMS. Under the above optimized conditions, all the AgNPs species were nearly baseline separated by the proposed hyphenated system (R_s > 1.5). In particular, the t_R of AgNPs increased with the increase of the diameter, and the particle size distribution of AgNPs could be evaluated by its peak shape in the fractogram. It is noteworthy that the broad peak of 10 nm AgNPs indicates the existence of smaller AgNPs, agreeing with the 4−6 nm AgNPs identified by TEM (Supporting Information, Figure S1B). Similarly, the TEM image depicted that the nominal 20 nm AgNPs (Supporting Information, Figure S1C) have a mean diameter of 16.9 nm, with a certain amount of smaller AgNPs with mean diameter of 9.8 nm that lead to somewhat overlapped peaks of 10 and 20 nm in the fractogram of the mixture. No significant peak was detected during the focusing time (t_R < 4 min) in the elution profile of the four commercial AgNPs studied (Figure 3), suggesting the absence of tiny AgNPs of <2 nm, which agreed with the TEM observation (Figure S1B−E).

Characterization of Particle Size. Figure 4A shows the UV−vis recording profiles of the four AgNPs, and the three PS NPs (nominal particle sizes of 22 ± 2 nm, 46 ± 2 nm, and 100 ± 3 nm) that are commonly used as size standards in particle analysis. Since the t_R of a particle is dependent on its hydrodynamic diameter in flow FFF, the particle sizes of the four AgNPs can be calibrated based on their t_R values, and the standard curve can be prepared by plotting the particle sizes against the t_R values of the PS NPs. Additionally, the particle sizes of the four AgNPs were determined by the on-line coupled DLS, and off-line counted from the TEM images. Therefore, three plots of the diameter against t_R of the four AgNPs were prepared, using the diameters obtained from calibration by the PS NP diameter, characterization by TEM, and direct measurement by on-line HF5-DLS, respectively (Figure 4B). All the correlation coefficients of the linear regression curves were better than 0.995, and as expected, the hydrodynamic diameters recorded by the on-line DLS detector were slightly larger than the diameters counted from the TEM images. The slope ratio of the plot of the TEM-based diameter to that of the PS NP-based diameter was 0.998, demonstrating the high accuracy in characterization of AgNPs size in aqueous samples using the proposed HF5/MCC-UV/DLS/ICPMS system. Given the low sensitivity in UV−vis and DLS detection, the plot of TEM-based diameter against retention time of the four AgNPs can be adopted as the standard curve to quantify the particle size of silver-containing NMs.

Quantification of Seven Ag Species. Seven Ag species, including Ag(I), Ag-Cys, and five species of AgNPs with nominal diameter of 1.4, 10, 20, 40, and 60 nm, were quantified based on the ICPMS response. Under the above optimized conditions, Ag(I), Ag-Cys, and 10 and 20 nm AgNPs in the concentration range of 5−5000 μg/L and 40 and 60 nm AgNPs in the concentration range of 10−5000 μg/L were determined by the developed method. As can been seen in Table 2, correlation coefficients for the seven linear regression curves (r) were no less than 0.989, suggesting their applicability in a relatively wide concentration range. The limit of detection (LOD), defined as three times the standard deviation of the

DOI: 10.1021/acs.analchem.5b01827
Anal. Chem. 2015, 87, 8441−8447

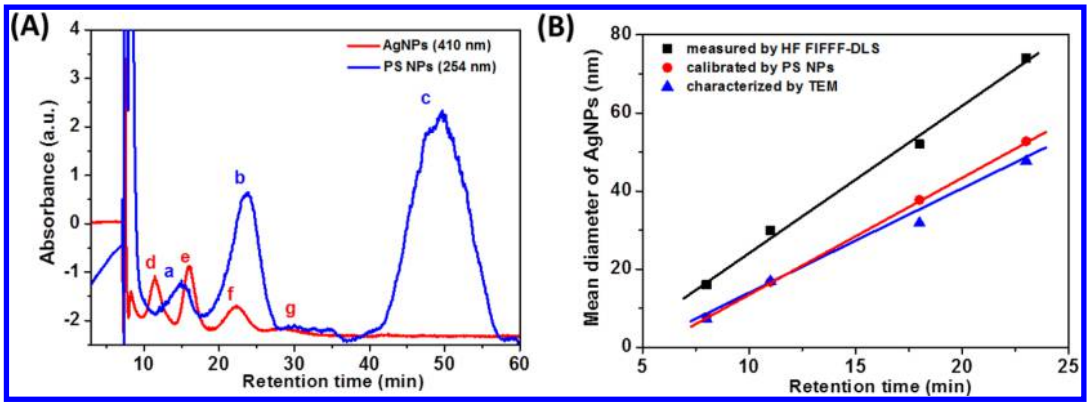

Figure 4. Size characterization of AgNPs. (A) Fractogram of AgNPs and PS NPs recorded with UV−vis detector. Peak assigment: a, 22 ± 2 nm PS NPs; b, 46 ± 2 nm PS NPs; c, 100 ± 3 nm PS NPs; d, 10 nm AgNPs; e, 20 nm AgNPs; f, 40 nm AgNPs; g, 60 nm AgNPs. (B) Plot of retention time against mean diameters of AgNPs measured by HF5-DLS, calibrated by PS NPs, and characterized by TEM, respectively. Experimental conditions: samples, PS NPs mixture (10 mg/L), and AgNPs mixture (1.0 mg/L); sample volume, 100 μL; mobile phase, 0.1% (v/v) FL-70 with 0.02% (w/v) NaN_3; inlet flow rate, 1.50 mL/min; radial flow rate, 0.70 mL/min; axial flow, 0.80 mL/min; focusing time, 4 min.

Table 2. Linear Ranges, r, LOD, and RSD for Determination of Various Ag Species by the Proposed Procedure

Ag species	Linear ranges (μg/L)	r	LOD (μg/L)	RSD[a] (%)
Ag(I)	5−5000 μg/L	0.993	1.6	4.2
Ag-Cys	5−5000 μg/L	0.998	1.3	1.9
AgNPs (1.4 nm)	5−5000 μg/L	0.989	1.7	5.8
AgNPs (10 nm)	5−5000 μg/L	0.995	1.2	5.3
AgNPs (20 nm)	5−5000 μg/L	0.992	1.4	4.6
AgNPs (40 nm)	10−5000 μg/L	0.993	2.9	5.7
AgNPs (60 nm)	10−5000 μg/L	0.990	3.2	6.3

[a]RSD was obtained by five measurements of peak area for seven Ag species at 50 μg/L.

background noise (S/N = 3), was in the range of 1.2−3.2 μg/L. Relative standard deviations (RSD) ranging from 1.9−6.3% demonstrated satisfactory repeatability.

Real Sample Characterization and Quantification. As all of the Ag species concentrations studied in the real water samples collected were found to be below their LODs, the applicability of the proposed method in real sample analysis was evaluated by assaying them in the spiked lake and river samples. The t_R values of the AgNPs in the spiked samples were nearly identical with that in working solutions (data not shown), indicating no significant difference in particle size. The Ag(I) content in AgNPs solution, determined by ICPMS after ultrafiltration (see procedures in Supporting Information), was 1% of total Ag; thus, Ag(I) sourced from the AgNPs solution was not accounted for in calculation of the Ag(I) recovery. Table 3 shows that recoveries of the spiked Ag species were in the range of 70.7−108%, demonstrating the applicability of the developed system in speciation analysis of Ag(I) and AgNPs in real water samples.

CONCLUSIONS

We have developed an on-line coupled HF5/MCC-UV/DLS/ICPMS system for full spectrum speciation analysis and characterization of different sized AgNPs and Ag(I). The HF5 coupled with a minicolumn packed with Amberlite IR120 resin successfully provides nearly baseline separation of free Ag(I) or weak Ag(I) complexes, strong Ag(I) complexes, and different sized AgNPs. Among them, the tiny AgNPs (<2 nm) could be identified and quantified by the decrement of the detected Ag amount in the focusing step through introducing diluted H_2O_2 in a second run. Using the multiple detectors, identification of Ag(I) and AgNPs, characterization of AgNPs, and quantification of Ag(I) and AgNPs can be achieved. Characterization results of AgNPs by the proposed method agreed well with that by TEM. The success of the developed method was also demonstrated by the good recoveries of Ag(I), Ag-Cys, and five species of AgNPs (1.4, 10, 20, 40, and 60 nm) determined in two spiked surface water samples. The proposed method is promising for studying the fate and transformation of AgNPs and Ag(I), as well as other engineered NPs in real environments.

Table 3. Concentration and Recovery of Seven Ag Species in Spiked Surface Water Samples Determined by the Proposed Procedure (mean ± SD, n = 3)

		Found in samples (μg/L)		Recovery (%)	
Ag species	Spiked (μg/L)	Lake water	River water	Laker water	River water
Ag(I)	10	10.8 ± 0.7	7.4 ± 0.5	108 ± 7	73.5 ± 5.4
Ag-Cys	10	8.1 ± 0.4	8.9 ± 0.2	81.5 ± 3.5	88.8 ± 2.3
AgNPs (1.4 nm)	10	9.3 ± 0.4	8.7 ± 0.5	92.9 ± 3.7	87.4 ± 5.1
AgNPs (10 nm)	10	8.3 ± 0.2	7.1 ± 0.3	83.6 ± 2.1	71.1 ± 3.4
AgNPs (20 nm)	10	9.8 ± 0.5	9.2 ± 0.7	97.8 ± 5.1	92.1 ± 7.1
AgNPs (40 nm)	20	16.3 ± 1.1	14.8 ± 0.9	81.6 ± 5.5	73.9 ± 4.6
AgNPs (60 nm)	20	15.6 ± 1.2	14.1 ± 0.7	77.9 ± 5.8	70.7 ± 3.4

DOI: 10.1021/acs.analchem.5b01827
Anal. Chem. 2015, 87, 8441−8447

■ ASSOCIATED CONTENT

Supporting Information

The Supporting Information is available free of charge on the ACS Publications website at DOI: 10.1021/acs.analchem.5b01827.

Preparation of GSH-protected Ag nanoclusters (GSH-Ag NCs), procedures for determination of Ag(I) and total Ag, TEM micrographs and respective histograms showing the size-distribution of GSH-Ag NCs prepared and four commercial AgNPs, influence of FL-70 concentration on separation resolution of AgNPs (10 nm and 20 nm), influence of the radial flow rate on ICPMS responses and separation resolution of AgNPs (10 nm and 20 nm), influence of the focusing time on ICPMS responses and separation resolution of AgNPs (10 nm and 20 nm), influence of axial flow rate on separation resolution of AgNPs (10 nm and 20 nm), and influence of sample volume on separation resolution of AgNPs (10 nm and 20 nm) (PDF)

■ AUTHOR INFORMATION

Corresponding Author

*Phone/Fax: +86-10-62849192. E-mails: jfliu@rcees.ac.cn.

Notes

The authors declare no competing financial interest.

■ ACKNOWLEDGMENTS

This work was supported by the Instrumentation Program Supported by the Chinese Academy of Sciences (YZ201147), the National Basic Research Program of China (2015CB932003), and the National Natural Science Foundation of China (21207141, 21227012, 21337004).

■ REFERENCES

(1) Nel, A.; Xia, T.; Madler, L.; Li, N. *Science* **2006**, *311*, 622−627.
(2) Panyala, N. R.; Pena-Mendez, E. M.; Havel, J. *J. Appl. Biomater.* **2008**, *6*, 117−129.
(3) Han, X. L.; Lai, L.; Tian, F. F.; Jiang, F. L.; Xiao, Q.; Li, Y.; Yu, Q. Y.; Li, D. W.; Wang, J.; Zhang, Q. M.; Zhu, B. F.; Li, R.; Liu, Y. *Small* **2012**, *8*, 2680−2689.
(4) Navarro, E.; Piccapietra, F.; Wagner, B.; Marconi, F.; Kaegi, R.; Odzak, N.; Sigg, L.; Behra, R. *Environ. Sci. Technol.* **2008**, *42*, 8959−8964.
(5) Lok, C. N.; Ho, C. M.; Chen, R.; He, Q. Y.; Yu, W. Y.; Sun, H. Z.; Tam, P. K. H.; Chiu, J. F.; Che, C. M. *J. Proteome Res.* **2006**, *5*, 916−924.
(6) Geranio, L.; Heuberger, M.; Nowack, B. *Environ. Sci. Technol.* **2009**, *43*, 8113−8118.
(7) Fabrega, J.; Fawcett, S. R.; Renshaw, J. C.; Lead, J. R. *Environ. Sci. Technol.* **2009**, *43*, 7285−7290.
(8) Wiesner, M. R.; Lowry, G. V.; Casman, E.; Bertsch, P. M.; Matson, C. W.; Di Giulio, R. T.; Liu, J.; Hochella, M. F. *ACS Nano* **2011**, *5*, 8466−8470.
(9) Quadros, M. E.; Pierson, R.; Tulve, N. S.; Willis, R.; Rogers, K.; Thomas, T. A.; Marr, L. C. *Environ. Sci. Technol.* **2013**, *47*, 8894−8901.
(10) Zhang, W.; Yao, Y.; Sullivan, N.; Chen, Y. S. *Environ. Sci. Technol.* **2011**, *45*, 4422−4428.
(11) Liu, J. Y.; Hurt, R. F. *Environ. Sci. Technol.* **2010**, *44*, 2169−2175.
(12) Yin, Y. G.; Liu, J. F.; Jiang, G. B. *ACS Nano* **2012**, *6*, 7910−7919.
(13) Yu, S. J.; Yin, Y. G.; Chao, J. B.; Shen, M. H.; Liu, J. F. *Environ. Sci. Technol.* **2014**, *48*, 403−411.
(14) Kaegi, R.; Voegelin, A.; Ort, C.; Sinnet, B.; Thalmann, B.; Krismer, J.; Hagendorfer, H.; Elumelu, M.; Mueller, E. *Water Res.* **2013**, *47*, 3866−3877.
(15) Choi, O.; Clevenger, T. E.; Deng, B. L.; Surampalli, R. Y.; Ross, L.; Hu, Z. Q. *Water Res.* **2009**, *43*, 1879−1886.
(16) Liu, J. Y.; Sonshine, D. A.; Shervani, S.; Hurt, R. H. *ACS Nano* **2010**, *4*, 6903−6913.
(17) Liu, W.; Wu, Y. A.; Wang, C.; Li, H. C.; Wang, T.; Liao, C. Y.; Cui, L.; Zhou, Q. F.; Yan, B.; Jiang, G. B. *Nanotoxicology* **2010**, *4*, 319−330.
(18) Shen, M. H.; Zhou, X. X.; Yang, X. Y.; Chao, J. B.; Liu, R.; Liu, J. F. *Sci. Rep.* **2015**, *5*, 9674.
(19) Liu, J. F.; Yu, S. J.; Yin, Y. G.; Chao, J. B. *TrAC, Trends Anal. Chem.* **2012**, *33*, 95−106.
(20) Jamison, J. A.; Krueger, K. M.; Mayo, J. T.; Yavuz, C. T.; Redden, J. J.; Colvin, V. L. *Nanotechnology* **2009**, *20*, 355702.
(21) Liu, J. F.; Chao, J. B.; Liu, R.; Tan, Z. Q.; Yin, Y. G.; Wu, Y.; Jiang, G. B. *Anal. Chem.* **2009**, *81*, 6496−6502.
(22) Liu, J. F.; Liu, R.; Yin, Y. G.; Jiang, G. B. *Chem. Commun.* **2009**, 1514−1516.
(23) Soto-Alvaredo, J.; Montes-Bayon, M.; Bettmer, J. *Anal. Chem.* **2013**, *85*, 1316−1321.
(24) Zhou, X. X.; Liu, R.; Liu, J. F. *Environ. Sci. Technol.* **2014**, *48*, 14516−14524.
(25) Liu, L. H.; He, B.; Liu, Q.; Yun, Z. J.; Yan, X. T.; Long, Y. M.; Jiang, G. B. *Angew. Chem., Int. Ed.* **2014**, *53*, 14476−14479.
(26) Pettibone, J. M.; Gigault, J.; Hackley, V. A. *ACS Nano* **2013**, *7*, 2491−2499.
(27) Bai, L.; Ma, X. J.; Liu, J. F.; Sun, X. M.; Zhao, D. Y.; Evans, D. G. *J. Am. Chem. Soc.* **2010**, *132*, 2333−2337.
(28) Liu, F. K. *J. Chromatogr. A* **2009**, *1216*, 9034−9047.
(29) von der Kammer, F.; Ferguson, P. L.; Holden, P. A.; Masion, A.; Rogers, K. R.; Klaine, S. J.; Koelmans, A. A.; Horne, N.; Unrine, J. M. *Environ. Toxicol. Chem.* **2012**, *31*, 32−49.
(30) Lee, W. J.; Min, B. R.; Moon, M. H. *Anal. Chem.* **1999**, *71*, 3446−3452.
(31) van Bruijnsvoort, M.; Kok, W. T.; Tijssen, R. *Anal. Chem.* **2001**, *73*, 4736−4742.
(32) Lee, H. L.; Reis, J. F. G.; Dohner, J.; Lightfoot, E. N. *AIChE J.* **1974**, *20*, 776−784.
(33) Jönsson, J. A.; Carlshaf, A. *Anal. Chem.* **1989**, *61*, 11−18.
(34) Kang, D.; Moon, M. H. *Anal. Chem.* **2005**, *77*, 4207−4212.
(35) Reschiglian, P.; Zattoni, A.; Cinque, L.; Roda, B.; Dal Piaz, F.; Roda, A.; Moon, M. H.; Min, B. R. *Anal. Chem.* **2004**, *76*, 2103−2111.
(36) Zhu, R. H.; Frankema, W.; Huo, Y. L.; Kok, W. T. *Anal. Chem.* **2005**, *77*, 4581−4586.
(37) Zattoni, A.; Rambaldi, D. C.; Casolari, S.; Roda, B.; Reschiglian, P. *J. Chromatogr. A* **2011**, *1218*, 4132−4137.
(38) Poda, A. R.; Bednar, A. J.; Kennedy, A. J.; Harmon, A.; Hull, M.; Mitrano, D. M.; Ranville, J. F.; Steevens, J. *J. Chromatogr. A* **2011**, *1218*, 4219−4225.
(39) Hoque, M. E.; Khosravi, K.; Newman, K.; Metcalfe, C. D. *J. Chromatogr. A* **2012**, *1233*, 109−115.
(40) Mitrano, D. M.; Barber, A.; Bednar, A.; Westerhoff, P.; Higgins, C. P.; Ranville, J. F. *J. Anal. At. Spectrom.* **2012**, *27*, 1131−1142.
(41) Ibrahim, T.; Battu, S.; Cook-Moreau, J.; Cardot, P. *J. Chromatogr. B: Anal. Technol. Biomed. Life Sci.* **2012**, *901*, 59−66.
(42) Laborda, F.; Bolea, E.; Jimenez-Lamana, J. *Anal. Chem.* **2014**, *86*, 2270−2278.
(43) Snyder, L. R.; Kirkland, J. J. In *Introduction to Modern Liquid Chromatography*, 2nd ed.; John Wiley & Sons: New York, 1979; pp 34−36.
(44) Carlshaf, A.; Jönsson, J. A. *J. Microcolumn Sep.* **1991**, *3*, 411−416.
(45) Fabricius, A. L.; Duester, L.; Meermann, B.; Ternes, T. A. *Anal. Bioanal. Chem.* **2014**, *406*, 467−479.

DOI: 10.1021/acs.analchem.5b01827
Anal. Chem. 2015, 87, 8441−8447